Monthly Notices
of the
ROYAL ASTRONOMICAL SOCIETY

MNRAS **439,** 1028–1037 (2014)
Advance Access publication 2014 February 5

doi:10.1093/mnras/stu026

Solar analogues and solar twins in the HARPS archive★

Juliet Datson,[1]† Chris Flynn[2,3,4] and Laura Portinari[1]

[1]*Tuorla Observatory, Department of Physics and Astronomy, University of Turku, Finland*
[2]*Centre for Astrophysics and Supercomputing, Swinburne University of Technology, VIC 3122 Australia*
[3]*Finnish Centre for Astronomy with ESO, University of Turku, FI-21500 Piikkio, Finland*
[4]*Department of Physics and Astronomy, University of Sydney, NSW 2006 Australia*

Accepted 2014 January 6. Received 2013 December 21; in original form 2013 November 5

ABSTRACT

We present 63 solar analogues and twins for which high signal-to-noise ratio (S/N) archival data are available for the High Accuracy Radial velocity Planet Searcher (HARPS) high-resolution spectrograph at the European Southern Observatory (ESO) 3.6-m telescope. We perform a differential analysis of these stellar spectra relative to the solar spectrum, similar to previous work using ESO 2.2-m/fiber-fed extended range optical spectrograph (FEROS) data, and expand our analysis by introducing a new method to test the temperature and metallicity calibration of Sun-like stars in the Geneva–Copenhagen Survey (GCS). The HARPS data are significantly better than the FEROS data, with improvements in S/N, spectral resolution and number of lines we can analyse. We confirm the offsets to the photometric scale found in our FEROS study. We confirm three solar twins found in the FEROS data as solar twins in the HARPS data, as well as identify six new twins.

Key words: stars: abundances – stars: fundamental parameters – stars: solar-type.

1 INTRODUCTION

This is the era of large stellar surveys of the Milky Way, with the aim of producing homogeneous catalogues of the kinematical and physical properties of very large numbers of stars, from $\sim 10^5$ in HERMES/GALAH (Freeman 2010) and the *Gaia*-ESO (European Southern Observatory; Gilmore et al. 2012) survey, through to the $\sim 10^9$ stars to be observed by *GAIA* (*GAIA*; Munari 2003). The basis for this ambitious surveying has its roots in the highly successful *Hipparcos* mission in the 1990s (Perryman et al. 1997; van Leeuwen 2007), and Two-Micron All-Sky Survey (2MASS; Skrutskie et al. 1995), and Sloan Digital Sky Survey (SDSS; York et al. 2000) in the early 2000s.

The estimation of precise and accurate physical parameters for these stars is crucially important for the investigation of a wide range of questions about the Milky Way, such as its chemical evolution, the stellar mass and luminosity functions, secular heating and radial migration of stars in the disc, and its star formation history.

The Geneva–Copenhagen Survey (GCS; Nordström et al. 2004; Holmberg, Nordström & Andersen 2007, 2009) is the largest effort to date in this direction. Surveying some 14 000 F, G and K dwarf stars in the solar neighbourhood, it has been used to examine a wide range of problems – from determining structures in the Milky Way (e.g. Famaey et al. 2005; Kaempf, de Boer & Altmann 2005), over abundance analysis of different stellar populations (e.g. Luck & Heiter 2005), all the way to characterizing planet host stars (e.g. Sozzetti 2004). The stellar physical parameters, primarily effective temperature, metallicity and stellar ages, are estimated from parallaxes and a careful calibration of the Strömgren indices. Since different photometric (or spectroscopic) techniques can differ by up to 100 K in temperature and 0.1 dex in metallicity, it is important to have independent ways to gauge a calibration.

In the previous work, Datson, Flynn & Portinari (2012, hereafter Paper I), inspired by standard techniques to select spectroscopic solar twins, we introduced new methods to test a temperature and metallicity scale with respect to the solar pinpoint. We performed a differential comparison of the strength of 109 weak, isolated lines in ∼100 stars, selected to be as Sun-like as possible from the GCS catalogue, relative to a solar reflection spectrum from the asteroid Ceres. We found, using fiber-fed extended range optical spectrograph (FEROS; Kaufer et al. 1999) data taken at the ESO/Max-Planck-Gesellschaft (MPG) 2.2-m telescope, that the GCS temperature and metallicity scales appear offset relative to the Sun by -97 ± 35 K and -0.12 ± 0.02 dex, respectively, similar to a finding made independently by Casagrande et al. (2010).

Very high signal-to-noise ratio (S/N) and high-resolution data for many of the GCS stars are available in the High Accuracy Radial velocity Planet Searcher (HARPS; Mayor et al. 2003) archive of the ESO 3.6-m telescope, taken as part of the programme to measure radial velocities of bright F, G and K stars in the search for stars which host planets.

In this paper, we have used HARPS data for 63 GCS stars found in the archive, to examine with high precision this potential offset

★Based in observations from the ESO Science Archive Facility: http://archive.eso.org/cms.html.

† E-mail: juliet.datson@utu.fi

in the GCS temperature and metallicity scale. We introduce a new method to measure the offsets, as well as adapt some of the same methods we developed for Paper I to this higher resolution and much higher S/N data. We anticipate that, although we have so far focused on the GCS catalogue, the differential comparison approach we have developed can be used to test the zero-point of the temperature and metallicity scale in any survey.

This large sample of solar analogues in the HARPS archive also allowed us to further search for solar twins – the best ones identified to date being 18 Sco (HD146233) and HIP56948 (HD101364) (Meléndez & Ramírez 2007; Bazot et al. 2011, 2012; Meléndez et al. 2012, Paper I) – which we determined through the use of some of the methods we developed in Paper I, but also introduce a new method; all are based on differential comparisons of our target stars to an asteroid spectrum, which serves as our stand-in solar spectrum.

We organize the paper as follows. In Section 2 we describe how we selected solar analogues in the HARPS archive and describe the data reduction. In Section 3 we present our analysis procedure to test the GCS catalogue calibration: a new method to compare stellar versus solar spectra, along with our previous methods from Paper I. In Section 4 we then use these methods to find solar twins in our data. Finally in Section 5 we summarize and draw our conclusions.

2 CANDIDATE SELECTION AND DATA REDUCTION

We have selected our solar analogues, as we did in Paper I, by choosing stars from the GCS-III (Holmberg et al. 2009, i.e. the latest version of the catalogue) which bracket the solar colour $(b-y)$ in the Strömgren system, absolute visual magnitude M_V and metallicity. We adopted the solar values of $(b-y)_\odot = 0.403$ (Holmberg, Flynn & Portinari 2006), $M_V = 4.83$ (Allen 1976) and [Fe/H] = 0.0 (by definition), and select stars in the ranges: $0.371 < (b-y) < 0.435$ in colour, $4.63 < M_V < 5.03$ in absolute magnitude and $-0.25 <$ [Fe/H] < 0.15 in metallicity. Note that the metallicity window is asymmetric, extended at the metal-poor end, to allow for the possible metallicity offset of −0.1 dex in the GCS scale, as found in Paper I.

We have searched the data archive of the HARPS (Mayor et al. 2003) at the ESO 3.6-m telescope at La Silla, finding 85 of our GCS stars which satisfy the above criteria and for which there is publicly accessible data in HARPS. We excluded two stars with highly broadened spectral lines (HD45270 and HD118072) which made it difficult for us to compare them to our solar spectrum. These stars have very high rotation values, their $v \sin i$ being 17.6 km/s and 21.4 km/s, respectively (Torres et al. 2006), whereas the Sun's value is only 2.29 km/s (Takeda et al. 2010). This left us with a sample of 83 stars, most of which had been observed many times with HARPS, allowing us to estimate our internal errors very well. We obtained a total of 408 spectra for our 83 stars, with S/N values in the range 30 to 450.

The spectra were acquired from 2003 to 2011. HARPS is an echelle spectrograph, with a resolution of $R \sim 115\,000$ and covering a spectral range of 3780–6910 Å. As a consequence, HARPS covers a smaller wavelength range than our FEROS (3500–9200 Å) observations in Paper I, but offers more than twice the resolution of FEROS (which is $R \sim 48\,000$). This allowed us to triple the number of atomic lines compared to what we used in Paper I.

We found a single Ceres spectrum for use as our reflected solar spectrum in the HARPS archive. We found other asteroid spectra as well as the Jovian moon Ganymede in the archive. Comparing these spectra with Ceres showed that there were no systematic differences in the equivalent widths (EWs) of the spectral lines: in other words, they yield good solar reflection spectra too, for all spectral lines used in our analysis. The Ceres spectrum was the best in terms of having the highest S/N (∼220) and is our solar standard throughout this paper.

An asteroid or Jovian moon necessarily reflects the spectrum of the Sun close to its equatorial plane, whereas stars are observed at random angles to this plane. Reassuringly, Kiselman et al. (2011) have shown that this has no significant effect on the EWs of the observed spectral lines, by comparing those determined from the Sun, taken at different position angles.

The HARPS pipeline provides what are essentially science-ready spectra. They had been corrected for the effects of the CCD bias, dark current, flat-fielding and cosmic rays. The spectra were then extracted and rebinned to 0.01 Å linear resolution. The wavelength calibration is based on Thorium lines from arcs, taken each afternoon.

The extracted 1D spectra showed broad wiggles in the continuum levels. These could be quite straightforwardly corrected out using the same approach as in Paper I for similar wiggles in the FEROS data. We made piecewise estimates of the continuum levels in 10-Å sections of the spectra and normalized them by linear fitting. This resulted, as in Paper I, in very flat spectra, in particular around the weak spectral lines for which we aimed to measure EWs.

3 DIFFERENTIAL ANALYSIS OF EQUIVALENT WIDTHS

Our analysis is based on a differential comparison between the spectra of the target stars and the reference solar spectrum. We used the same program, TWOSPEC, as in Paper I, to measure EWs of lines for a wide range of species, both neutral and ionized, and measure the median difference for these species in the star compared to the Sun (see Paper I for full details on TWOSPEC). We adapted the line list from Bensby, Feltzing & Lundström (2003) for our resolution and wavelength range for use with our HARPS data. This resulted in a list three times as long as the one used in Paper I, i.e. 321 weak, unblended lines from 10 different elements (Na, Mg, Al, Si, Ca, Ti, Cr, Fe, Ni and Zn), six of which have lines from the ionized as well as the neutral state. The list is available from the authors upon request.

In most of what follows we use the same methods as described in Paper I (but also introduce a new method – see Section 3.1) to test the temperature and metallicity calibration in the GCS catalogue for solar-type stars (this section) and to search for new twins (Section 4).

As before, our approach is to measure the median difference in EW of selected lines between the star's and the solar reference spectrum, relative to the EW in the Sun. For a solar twin, this quantity will vanish (to within the errors).

$$\langle \Delta \mathrm{EW} \rangle = \left\langle \frac{(\mathrm{EW}(*) - \mathrm{EW}(\odot))}{\mathrm{EW}(\odot)} \right\rangle . \quad (1)$$

We begin by examining the S/N distribution of our spectra and its effect on our measure of this quantity. This is shown in Fig. 1. For the test we considered Fe I lines, which are the most numerous in our line list.

Below a S/N of approximately 50, the scatter in the medians for multiple observations of the same star increases very significantly, and all spectra with S/N < 50 were removed from the sample. We

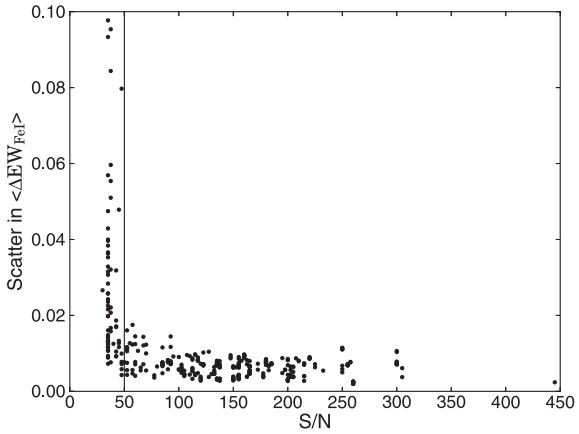

Figure 1. The scatter in the median difference in EW relative to the Sun, for all stars in our sample, as a function of the spectrum S/N. The scatter increases very significantly for S/N below 50 (solid line). These spectra have been dropped from our analysis.

have checked and confirm that the results of the paper do not change significantly if we impose a stricter S/N selection.

This culling left us with 329 spectra with $50 < S/N < 450$, for a total of 63 individual stars, of which 15 have been also observed in our FEROS sample of Paper I (including three solar twins) and thus allow a comparison with our earlier results.

3.1 The neutral-ionized (n/i) method

One way to disentangle temperature, metallicity and gravity effects on the lines in the spectra of Sun-like stars is to exploit the different sensitivities of the neutral versus the ionized lines of the same element.

We have searched the literature for lines of both ionization states (neutral and singly ionized) for as many species as possible for inclusion in our line list. The main source of lines is the work of Bensby et al. (2003), and includes reasonable numbers of lines from Fe, Ti, Ca, Ni, Cr and Si. We carefully examined our Ceres and other HARPS spectra, as we had done for FEROS, to remove any lines which were too weak (generally those with EWs < 15 mÅ) or had nearby lines which would make EW measurements unreliable. Far more lines could be used than for our FEROS data, as the spectral resolution of HARPS is a factor of more than 2 greater, and the final list contained 323 lines. Table 1 shows the final numbers of lines we have used for elements with lines in both ionization states.

Table 1. Numbers of lines used for each species in our neutral-ionized-method for finding Sun-like stars. The lines lie in the HARPS spectral range.

Element	Number of neutral lines	Number of ionized lines
Iron	126	25
Titanium	19	17
Calcium	22	4
Nickel	42	5
Chromium	9	3
Silicon	15	20

3.1.1 The technique

We ran TWOSPEC to compare the EWs of each element, in the stellar versus Ceres spectrum, separating the neutral and ionized lines, and define a median difference in EW for every element and each state:

$$\left\langle \Delta \mathrm{EW}_{\mathrm{n/i}} \right\rangle = \left\langle \frac{(\mathrm{EW}_{\mathrm{n/i}}(*) - \mathrm{EW}_{\mathrm{n/i}}(\odot))}{\mathrm{EW}_{\mathrm{n/i}}(\odot)} \right\rangle \quad (2)$$

with the subscripts n indicating neutral elements and i ionized elements.

In Figs 2–4, we show the median EW differences relative to the Sun for all stars in the sample, plotted as a function of the GCS values of T_{eff}, [Fe/H] and the absolute magnitude of the stars M_V, using the *Hipparcos* parallax, for all elements analysed (Fe, Ti, Ca, Ni, Cr and Si) for both neutral and ionized lines.

A particularly interesting example is Titanium. Looking at the case of Ti I and Ti II, we see correlations, anti-correlations and negligible correlation for all three stellar physical parameters probed. It turns out that very good fits for the measured median EW difference can be made by simply fitting a plane as a function of T_{eff} and [Fe/H], and only marginally improved fits made if we also include M_V as a linear term in the fitting:

$$\left\langle \Delta \mathrm{EW}_{\mathrm{n/i}} \right\rangle = a(T_{\mathrm{eff}} - T_{\mathrm{eff},\odot}) + b([\mathrm{Fe/H}] - [\mathrm{Fe/H}]_{\odot}) + c(M_V - M_{V,\odot}), \quad (3)$$

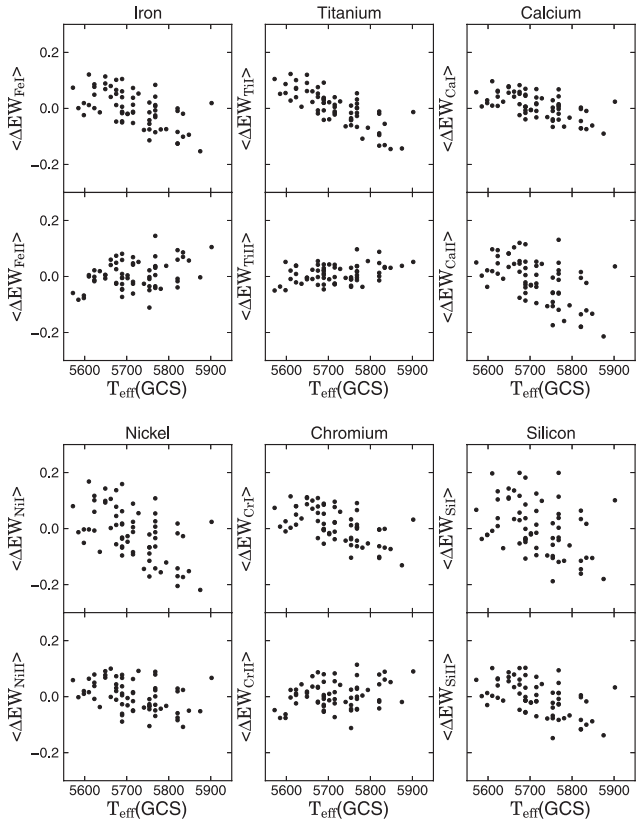

Figure 2. The median relative difference in EWs of the spectral lines as a function of the stellar temperature from the GCS catalogue, for Fe, Ti, Ca, Ni, Cr and Si. Upper panels in each plot show result for the neutral lines, and lower panels for the singly ionized lines. Correlations, anti-correlations and weak correlations are all seen in the plot. We exploit these different trends to probe for any offset in the temperature and metallicity scales of GCS relative to the Sun, and to isolate the most Sun-like stars in the sample.

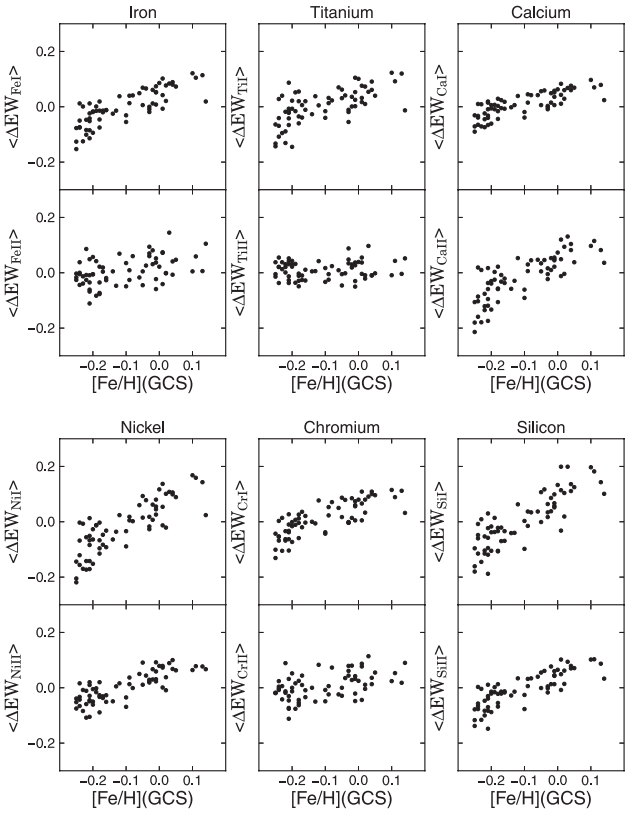

Figure 3. As for Fig. 2, but showing the trends versus the GCS metallicity of the stars.

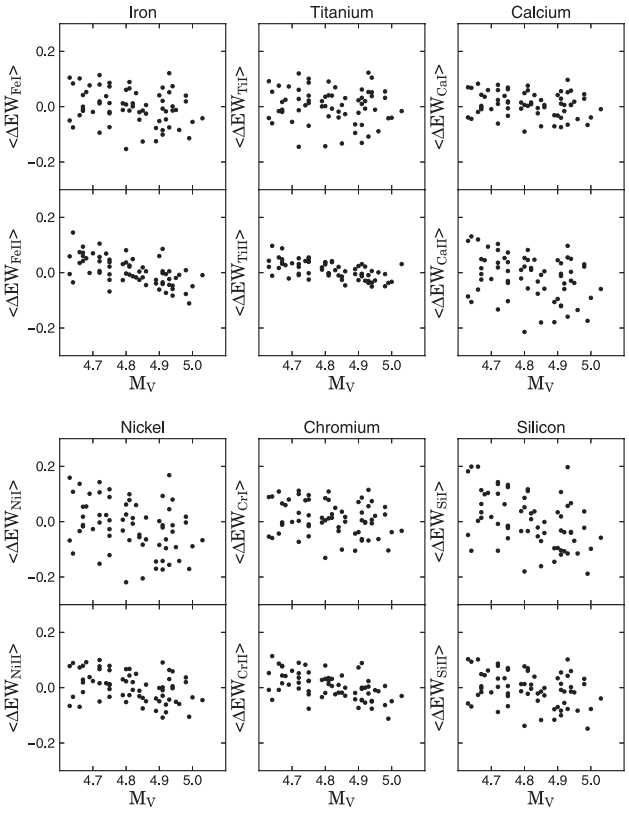

Figure 4. As for Fig. 2, but showing trends versus the absolute magnitude, M_V of the stars.

with $M_{V,\odot} = 4.83$ (Allen 1976) and temperature and metallicity values being those in the GCS-III catalogue.

This yields two equations for each element, one for the neutral lines and one for the ionized lines. Setting the left-hand side of each equation to zero, we can solve for any offset in the GCS temperature and metallicity calibrations.

The range of the absolute magnitude amongst our target stars is quite small – by design it is centred close to the solar value – and thus the range of surface gravities in the stars [i.e. $\log(g)$] is expected to be very small. Therefore we assume (and verify a posteriori; see below) its influence on our spectral lines to be small. So, by neglecting the M_V term in the above equations and rearranging, we find the two independent relationships for effective temperature and metallicity:

$$T_{\rm eff} = T_{\rm eff,\odot} + a\,\langle\Delta{\rm EW}_{\rm neutral}\rangle + b\,\langle\Delta{\rm EW}_{\rm ionized}\rangle \quad (4)$$

$$[{\rm Fe/H}] = [{\rm Fe/H}]_{\odot} + c\,\langle\Delta{\rm EW}_{\rm neutral}\rangle + d\,\langle\Delta{\rm EW}_{\rm ionized}\rangle \quad (5)$$

which explicitly shows that the solar values correspond to where both median differences, in neutral and ionized lines, vanish.

For each of the six elements considered, a 2D least-squares fit to the data in Figs 2 and 3 provides us with the coefficients in equations (4) and (5); the intercepts in particular correspond to the solar values for temperature and metallicity within the GCS.

Table 2 shows the results we get for this 2D fitting of the data.

We have tested the effect of neglecting the dependence of the EWs on absolute magnitude in equation (3). This corresponds to including a linear term in $(M_V - M_{V,\odot})$ to equations (4) and (5), and re-performing the least-squares fitting. We found the results were unchanged within the errors, along with negligible improvement in the χ^2 values of the fits. This shows that the dependencies on M_V in Fig. 4 are primarily driven by $T_{\rm eff}$ and [Fe/H] – that is, once we account for these two dependencies, there is no additional dependence of the $\langle\Delta EW\rangle$ on magnitude/gravity, at least not within the narrow selected magnitude range. There was an exception to this result however: for calcium, inclusion of an M_V dependency improved the fitting and provided zero-point values for temperature and metallicity more consistent with the values from the other elements (see Table 2).

In Fig. 5, the filled circles show the GCS solar temperature and metallicity values we obtain for each of the six elements analysed.

We thus confirm, with a larger and higher quality data set and a new method, our results from Paper I: the GCS temperature scale is offset by -60 ± 10 K and the metallicity scale by -0.11 ± 0.02 dex for solar-type stars, which agrees with our previous results from Paper I within the errors (-100 ± 40 K and -0.12 ± 0.02 dex, respectively).

3.1.2 The n/i-method: internal precision and performance using synthetic spectra

As in Paper I, our methods are novel and we have constructed several tests to check their performance.

Our first test is to randomly chose 20 stars from the sample as reference stars, instead of using Ceres (i.e. the solar spectrum), to determine how well the method recovers their catalogued temperatures and metallicities. We used the same procedures as in Section 3.1.1, but simply replace Ceres with the randomly chosen star. Some examples of results for a few stars tested are shown in Table 3.

We recover the input temperatures and metallicities of the stars very well, finding an average temperature offset of only $\Delta T_{\rm eff} = -7 \pm 40$ K and metallicity offset of only

Table 2. Estimated solar values for effective temperature and metallicity in the GCS calibration and the resulting $(b-y)$ colour of the Sun, determined through our (n/i) method.

Element	$T_{\rm eff,\odot}$ (K)	$a_{T_{\rm eff}}$	$b_{T_{\rm eff}}$	$[{\rm Fe/H}]_\odot$ (dex)	$c_{\rm [Fe/H]}$	$d_{\rm [Fe/H]}$	$(b-y)_\odot$	$e_{(b-y)}$	$f_{(b-y)}$
Iron	5713 ± 2	−964 ± 32	1049 ± 42	−0.104 ± 0.003	1.29 ± 0.05	0.54 ± 0.06	0.4093 ± 0.0002	0.199 ± 0.004	−0.147 ± 0.005
Titanium	5717 ± 2	−906 ± 31	794 ± 62	−0.113 ± 0.005	1.12 ± 0.07	0.82 ± 0.13	0.4084 ± 0.0002	0.184 ± 0.003	−0.096 ± 0.007
Calcium	5748 ± 5	−1861 ± 233	444 ± 125	−0.093 ± 0.006	0.49 ± 0.25	0.86 ± 0.14	0.4042 ± 0.0005	0.338 ± 0.024	−0.064 ± 0.015
Calcium 3D-fit	5729 ± 5			−0.110 ± 0.006			0.4065 ± 0.0007		
Nickel	5707 ± 4	−658 ± 64	486 ± 108	−0.088 ± 0.003	0.83 ± 0.06	0.33 ± 0.09	0.4108 ± 0.0005	0.135 ± 0.009	−0.066 ± 0.015
Chromium	5728 ± 2	−1097 ± 40	1059 ± 50	−0.120 ± 0.004	1.25 ± 0.06	0.54 ± 0.08	0.4063 ± 0.0003	0.218 ± 0.005	−0.149 ± 0.007
Silicon	5706 ± 3	1233 ± 100	2492 ± 157	−0.105 ± 0.003	0.92 ± 0.10	0.11 ± 0.15	0.4103 ± 0.0004	−0.159 ± 0.014	0.394 ± 0.023
Average	5717 ± 18			−0.11 ± 0.03			0.409 ± 0.002		

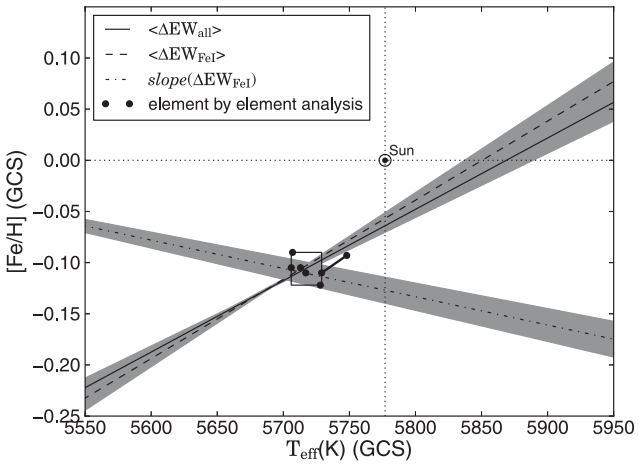

Figure 5. Filled circles show the resulting solar temperatures and metallicities from the neutral-ionized method. The two connected points show the two results for calcium. The lines show the trends from the degeneracy lines method (see Section 3.2). We also plot where the Sun lies in the GCS-III scale, as opposed to the location, where the degeneracy lines cross, which is where our method finds the most Sun-like stars in the sample.

Table 3. Results from stars used to test the (n/i) method, showing their GCS temperatures and metallicities and how close we are to recovering those by applying our method to all the remaining stars in the sample. Note that this is a self-consistency check of the method only.

Name	$T_{\rm eff}$ (GCS)	$\Delta T_{\rm eff}$ (fit-GCS)	[Fe/H] (GCS)	Δ[Fe/H] (fit-GCS)
HD 361	5821	−7	−0.25	−0.02
HD 4391	5741	20	−0.25	0.05
HD 13724	5675	5	0.01	0.04
HD 34449	5821	−45	−0.22	0.00
HD 59711	5715	6	−0.21	0.02
HD 67458	5875	−45	−0.25	−0.04
HD 78660	5715	−27	−0.09	−0.01
HD 114853	5754	−19	−0.21	−0.05
HD 126525	5585	84	−0.19	0.07
HD 146233	5768	−42	−0.02	−0.06

Δ[Fe/H] = 0.01 ± 0.04 dex between the input and output values for the 10 stars. This demonstrates that the method is internally highly consistent.

We have tried the same test using synthetic spectra rather than our observational material. We used the POLLUX model spectra by Palacios et al. (2010), selecting models which bracket the solar values of temperature (5500 K, 5750 K and 5600 K), metallicity (−0.50, −0.25, 0.00, +0.25 and +0.50) and gravity [log(g) = 4.0, 4.5 and 5.0]. We arbitrarily adopt one of the spectra as our 'solar' reference spectrum, and determine if we can recover its temperature and metallicity by applying our method to the rest of the stars. The reference spectrum we adopted was the model with $T_{\rm eff}$ = 5750 K, [Fe/H] = 0.00 dex and log(g) = 4.5. Although these spectra span the solar values rather widely and coarsely, we nevertheless found our method recovers the correct temperature and metallicity within the errors for the selected reference spectrum, yielding $T_{\rm eff}$ = 5757 ± 18 K and metallicity at [Fe/H] = −0.03 ± 0.03 dex.

We conclude from these internal consistency tests that our (n/i) method does indeed recover the parameters of the reference target.

3.2 The degeneracy lines method applied to HARPS data

For consistency and comparison to our previous work, we also apply our 'degeneracy lines' methods (i) and (ii) from Paper I. Method (i) is based on differential comparison of the EWs of 323 mostly neutral lines of 10 elements (Ti, Fe, Al, Ca, Cr, Mg, Na, Ni, Si and Zn), and method (ii) combines $\langle\Delta{\rm EW_{Fe\,I}}\rangle$ and slope of $\langle\Delta{\rm EW_{Fe\,I}}\rangle$ versus excitation potential of 129 Fe I lines. Because of the different telescopes and instruments, the line list we used this time is different from the one we used in Paper I. We decided not to use here the line depth versus excitation potential method [method (iii) in Paper I], which closely resembled method (ii) but using line depths instead of EWs: we found in Paper I that these methods are virtually indistinguishable, so we now consider method (iii) redundant.

We used our TWOSPEC code to determine the relevant quantities $\langle\Delta{\rm EW_{all}}\rangle$, $\langle\Delta{\rm EW_{Fe\,I}}\rangle$ and slope[$(\Delta{\rm EW_{Fe\,I}})$ versus $\chi_{\rm exc}$]. We made a 2D least-squares fit of these quantities to solve their combined dependency on metallicity and temperature (GCS values; see Fig. 6):

$$\langle\Delta{\rm EW_{all}}\rangle = 0.493[{\rm Fe/H}] - 1.986\left(\frac{T_{\rm eff}-5777}{5777}\right) + 0.032 \quad (6)$$

$$\langle\Delta{\rm EW_{Fe\,I}}\rangle = 0.511[{\rm Fe/H}] - 2.284\left(\frac{T_{\rm eff}-5777}{5777}\right) + 0.029 \quad (7)$$

$$\text{slope}[(\Delta{\rm EW_{Fe\,I}}) \text{ versus } \chi_{\rm exc}] = 0.519[{\rm Fe/H}] + 0.829\left(\frac{T_{\rm eff}-5777}{5777}\right) + 0.066. \quad (8)$$

The left-hand side of the three equations vanish for a perfect solar twin, so we can set the left-hand side to zero and invert the equations, yielding:

$$[{\rm Fe/H}]_{\langle\Delta{\rm EW_{all}}\rangle} = 4.028\left(\frac{T_{\rm eff}-5777}{5777}\right) - 0.064 \quad (9)$$

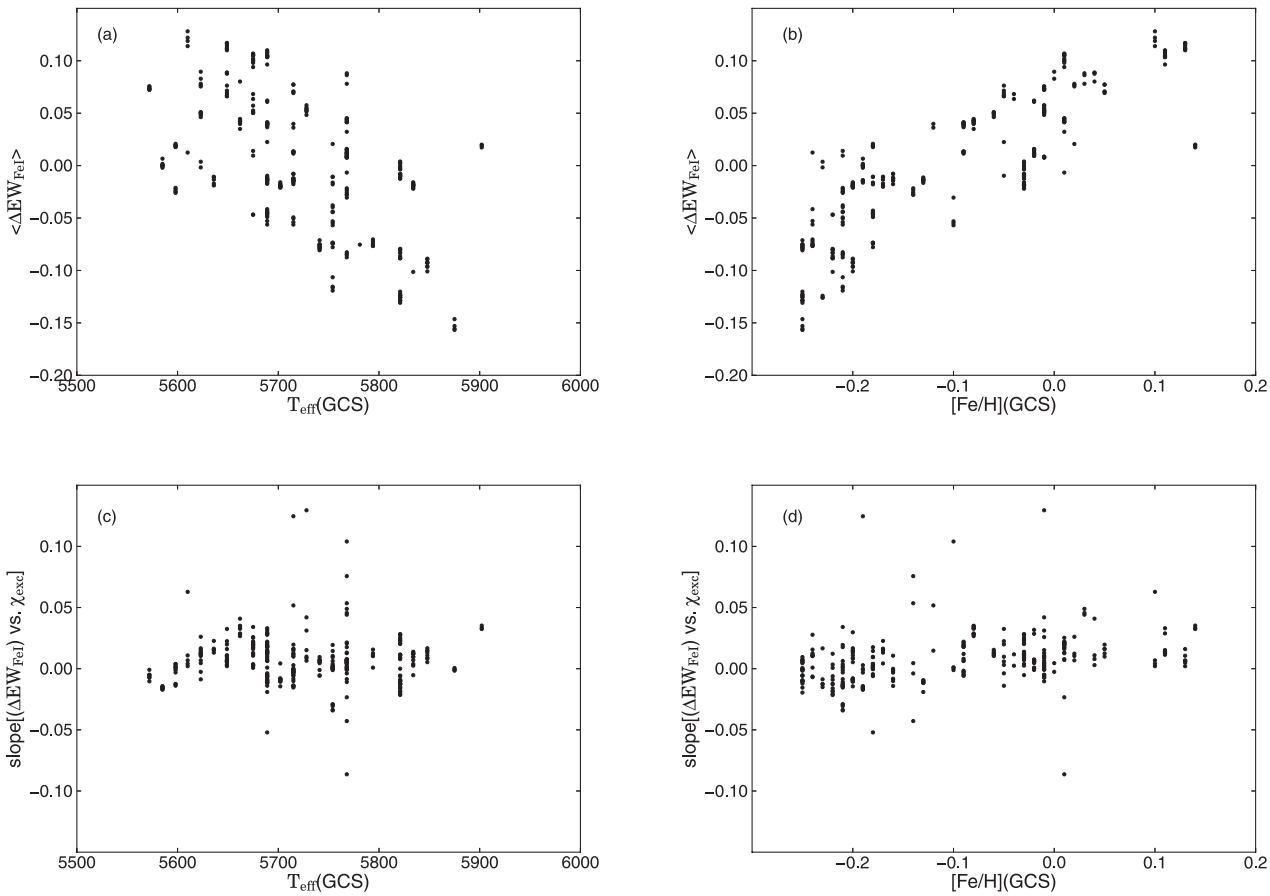

Figure 6. Panel (a): the median difference in EW of the neutral iron lines for all target stars, depending on their temperatures and their metallicities [Panel (b)]. Panel (c): the slopes of the relation between the median relative difference in EW as a function of the excitation potential of the line (details in Paper I); depending on temperature and [Panel (d)] metallicity. We use these trends in Section 3.2 to determine the offsets in temperature and metallicity in the GCS.

$$[\mathrm{Fe/H}]_{\langle \Delta \mathrm{EW_{Fe\,I}} \rangle} = 4.467 \left(\frac{T_{\mathrm{eff}} - 5777}{5777} \right) - 0.057 \tag{10}$$

$$[\mathrm{Fe/H}]_{\mathrm{slope}[(\Delta \mathrm{EW_{Fe\,I}}) \text{ versus } \chi_{\mathrm{exc}}]} = -1.598 \left(\frac{T_{\mathrm{eff}} - 5777}{5777} \right) - 0.127. \tag{11}$$

As in Paper I, we found the slope parameter to be almost completely independent of temperature (see Fig. 6a) although we formally kept the dependence in the equation, for consistency with the analysis of the scale of Casagrande et al. (2011, hereafter C11) in Section 3.3.

Plotting these relations in the metallicity–temperature plane, we find, as in Paper I, that they cross at a point offset from the solar values, by -0.10 ± 0.02 dex in metallicity and -50 ± 25 K in temperature (see Fig. 5).

It is possible that the strength of the our spectral lines may be introducing a bias into our method: to check this, we divided the lines into median strength ($\log(\frac{EW}{\lambda}) > -5$), and weak ($\log(\frac{EW}{\lambda}) < -5$); each sublist contains about half of the lines of the original full list. We find no change to the results when adopting each sublist in turn. Our list of solar twins, selected in Section 4 with similar methods, is also robust to this test.

3.3 The reanalysis of the GCS (C11)

C11 have analysed the GCS catalogue, using the InfraRed Flux Method on solar twins to set the temperature scale, and redetermining the physical parameters of the stars. They find their calibration to be ∼80 K hotter and ∼0.1 dex metal richer than in the GCS.

We have applied our method to their temperatures and metallicities, to check the zero-point of their scales relative to the Sun. We apply all the methods discussed above, and show the results in Fig. 7.

We find the solar values in C11 are at $T_{\mathrm{eff}} = 5790 \pm 15$ K and $[\mathrm{Fe/H}] = -0.02 \pm 0.02$ dex: this is very close to the accepted solar values, and so this work favours the C11 scales over the original one, at least for Sun-like stars (i.e. within a window of 250 K in temperature and 0.15 dex in metallicity around the Sun). We note this is not particularly surprising considering that the temperature scale of Casagrande et al. (2010) and C11 was explicitly calibrated on solar twins.

3.4 The solar $(b - y)$ colour

Analogous to Paper I, we applied the same procedures using the $(b - y)$ colour of the target stars instead of the temperature, to determine the solar $(b - y)$ colour. For this purpose we first fitted the following relation to our six different elements, as in our

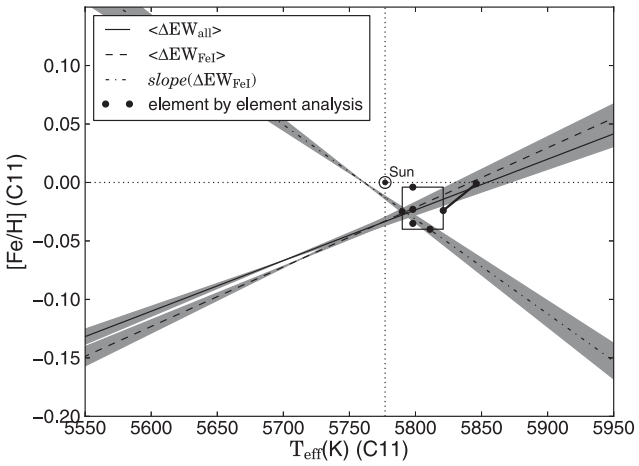

Figure 7. Same as Fig. 5, but using C11 values for temperature and metallicity. Again we also plot the position of the Sun in the C11 scale.

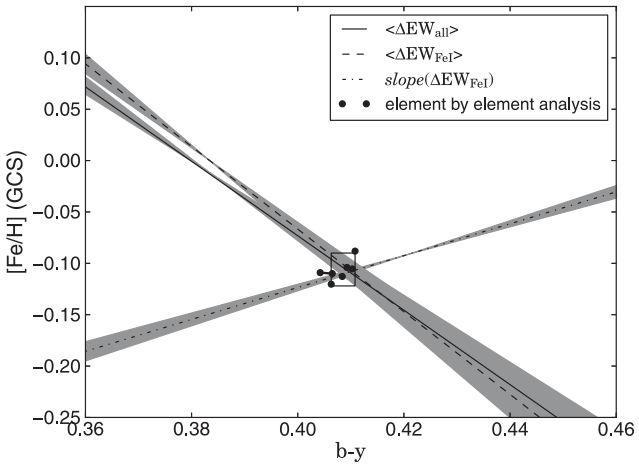

Figure 8. Same as Fig. 5, but looking at the $(b-y)$ colour instead of the temperature. The solar colour is derived from the crossing point of the relations and yields a $(b-y)_{\odot}$ colour of 0.409 ± 0.005.

(n/i)-method (see Section 3.1):

$$(b-y) = (b-y)_{\odot} + e\,\langle \Delta \mathrm{EW}_{\mathrm{neutral}} \rangle + f\,\langle \Delta \mathrm{EW}_{\mathrm{ionized}} \rangle\,. \qquad (12)$$

We then used the degeneracy lines method, as in Section 3.2, and derived an overall estimate for the solar $(b-y)$ colour of 0.409 ± 0.005 (Fig. 8 and Table 2).

This is very consistent with the results of Meléndez et al. (2010), who obtained $(b-y) = 0.4105 \pm 0.0015$ through Strömgren photometry and also with the value we found in Paper I: $(b-y) = 0.414 \pm 0.007$.

4 FINDING THE SOLAR TWINS FROM HARPS

As shown in Paper I, there are currently many different ways of selecting solar twins. The interested reader is referred to it for full details; we give short descriptions of each method in what follows.

We first use the median difference in EW of a list of spectral lines [Paper I, method (i)] and the median difference in EW of only the Fe I lines [Paper I, method (ii)].

We have also adapted the (n/i)-method from Section 3.1 of this paper, as another way to look for solar twins. This relies on finding the minimum of the median difference in EW of specific elements (Fe, Ti, Ca, Ni, Cr and Si) but separating the lines from the neutral species and the ones from the singularly ionized species; see method (n/i) (Section 4.3).

4.1 Method (i): the EWs of all 321 spectral lines

As shown in Paper I, this method [which is similar to the 'first criterion' method of Meléndez, Dodds-Eden & Robles (2006)], uses the median $\langle \Delta \mathrm{EW}_{\mathrm{all}} \rangle$ and scatter $\chi^2(\Delta \mathrm{EW}_{\mathrm{all}})$ of the differences $\Delta \mathrm{EW}_{\mathrm{all}}$ in the EWs of target stars relative to Ceres for all our lines, to determine a star's solar likeness.

To determine the errors in the measurements of our various parameters in methods (i) and (ii), we used the fact that we had many targets with several spectra. Comparing the measurements with one another resulted in the following error values: $\sigma(\chi^2(\Delta \mathrm{EW}_{\mathrm{all}})) = 0.1$, $\sigma(\langle \Delta \mathrm{EW}_{\mathrm{all}} \rangle) = 0.001$, $\sigma(\langle \Delta \mathrm{EW}_{\mathrm{Fe\,I}} \rangle) = 0.001$ and $\sigma(\mathrm{slope}(\Delta \mathrm{EW}_{\mathrm{Fe\,I}})$ versus $\chi_{\mathrm{exc}}) = 0.001$.

In Paper I the definition of a solar twin has been based on a match to the solar spectrum to within a limit defined by the observational scatter. We used the criterion that our twins should be solar within 2σ, where σ was the observational scatter, as determined from multiple measurements of the indicator used in each method. Our HARPS data are now so accurate that the same 2σ criterion yields no solar twins. We therefore adopt the following expedient: we define solar twins as being within 1 per cent of the Sun in the measured indicator. For the median method, the difference between the EW of the lines in the star and in the Sun should differ by less than 1 per cent of the solar value. Fig. 9 shows an overview on the range of values and the twin selection limits for this criterion.

Additionally we define the scatter to be only the observational scatter, in this case $\chi^2 \leq 1$. Thus we find five stars we consider to be solar twins, as shown in Table 4. The well-known twin 18 Sco lies just outside the limits with a $\langle \Delta \mathrm{EW}_{\mathrm{all}} \rangle$ of 1.2 per cent of solar.

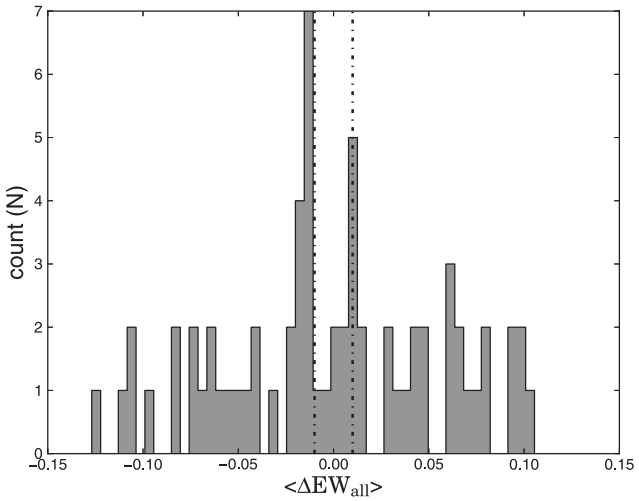

Figure 9. Histogram of the median relative difference in EWs for all lines $\langle \Delta \mathrm{EW}_{\mathrm{all}} \rangle$ in our sample. The broken lines show where we applied the 1 per cent cuts, thus every stellar spectrum within the lines are considered to be that of a solar twin.

Table 4. List of solar twins using $\chi^2(\Delta EW_{all})$ [i.e. method (i)], ordered by $\chi^2(\Delta EW_{all})$.

Name	$\chi^2(\Delta EW_{all})$	$\langle \Delta EW_{all} \rangle$
HD 19641	0.5 ± 0.1	−0.005 ± 0.001
HD 78660	0.5 ± 0.1	0.006 ± 0.001
HD 45184	0.6 ± 0.1	0.001 ± 0.001
HD 126525	0.9 ± 0.1	0.000 ± 0.001
HD 76440	1.0 ± 0.1	0.006 ± 0.001

Table 5. List of solar twins from method (ii).

Name	$\langle \Delta EW_{Fe\,I} \rangle$	Slope[$(\Delta EW_{Fe\,I})$ versus χ_{exc}]
HD 45184	−0.009 ± 0.001	0.009 ± 0.001
HD 76440	−0.001 ± 0.001	−0.009 ± 0.001
HD 78538	−0.008 ± 0.001	−0.007 ± 0.001
HD 146233	0.009 ± 0.001	0.007 ± 0.001
HD 183658	0.008 ± 0.001	0.001 ± 0.001

4.2 Method (ii): the EWs of 129 Fe I lines versus their excitation potential

This method, which we also adopted in Paper I, is originally inspired by the technique used by Meléndez & Ramírez (2007), where we use only the 129 Fe I lines in our line list. We determine the median $\langle \Delta EW_{Fe\,I} \rangle$ for these lines and the slope[$(\Delta EW_{Fe\,I})$ versus χ_{exc}], which should be zero for a solar twin.

Analogously to the previous section, we adopt the definition of a star being solar, when these values lie within 1 per cent of the solar values.

This gives us also five stars we can consider as solar twins (see Table 5), two of which also satisfied method (i): HD45184 and HD76440.

4.3 Method (n/i)

In addition to the previous criteria, which are the same as in Paper I, we introduce the new criterion inspired by our neutral/ionized lines method of Section 3.1, by considering a star to be a solar twin, if, for more than one element used in our analysis (Fe, Ti, Ca, Ni, Cr and Si), see Table 6, the following criterion holds:

$$|\langle \Delta EW_{neutral} \rangle| + |\langle \Delta EW_{ionised} \rangle| \leq 0.02. \quad (13)$$

This yields six twins, five of which have already been found to be twins in the previous sections, which shows the analysis is robust to changes in the twin definition. The sixth twin was only recently found to be the oldest twin known to date by Monroe et al. (2013) at an age of ∼8.2 Gyr.

Table 6. List of solar twins from method (n/i).

Name	Elements for which the criterion is fulfilled
HD 197027	Fe, Ni, Cr, Si
HD 76440	Fe, Ca, Ni, Si
HD 78660	Ca, Ni, Si
HD 19641	Ca, Cr
HD 126525	Ca, Ni
HD 146233	Ti, Ca

When comparing the abundances of different elements in the Sun to those in solar twins, Meléndez et al. (2009) showed that volatile elements are more abundant in the Sun, whereas refractory elements are either of similar or lower abundance. In our study this is in principle a concern for silicon, a volatile element whose relative abundance in Meléndez et al. (2009) is found to be about 0.03 dex higher than that of iron or of other refractory elements like Ti. In practice, we find no sign of this dichotomy in our results: in Section 3.1.1 there is no significant difference between the Si-based results of the n/i method versus other elements; and the solar twins we selected with the various methods are not peculiar, and very close to solar, in $\langle \Delta EW_{Si} \rangle$. We plan to return to this issue in the near future, with a detailed abundance analysis of our twins (from this paper and Paper I) based on UVES spectra.

4.4 Final list of solar twins

Looking at all three methods together, we classify the following stars as the solar twins in our sample (Table 7).

Only one star in our sample satisfies all three of our criteria: HD 76440. There are five stars which satisfy two of the criteria and three stars that satisfy one criterion.

Of the 10 solar twins we reported in Paper I from the FEROS data, three were found in the HARPS archive and included in our sample for this paper. All three here are also identified as twins, using the methods described above, which makes us confident in the robustness of our methods' end results, as we recovered the same, common twins with a different telescope, instrument, line list and method. These three stars are HD 78660, HD 126525 and HD 146233.

Of the nine stars we consider solar twins here, three have been previously published as twins in and before Paper I, HD 146233, HD 78660 and HD 126525; HD 197027 was only recently found to be an old twin (Monroe et al. 2013); the other five stars are completely new twins: HD 45184, HD 76440, HD 19641, HD 78538 and HD 183658.

In Fig. 10 we show where the twins lie in the colour–magnitude diagram, compared to the twins from Paper I.

To check to what extent the choice of line list used influences our results, we tested the effect of using the shorter FEROS line list from Paper I on the HARPS data, and also taking into account the reduced wavelength coverage of the HARPS spectra. Using this line list, with ∼100 lines, we recover four of the nine twins mentioned above, namely HD 45184, HD 76440, HD 126525 and HD 183658. Our methods are quite robust, as we recover the same twins for a broad range of comparison lines, species, ionization states, telescopes and instrumental resolutions.

Using the average properties of solar twins to check calibrations is a widely applied technique (Casagrande et al. 2010; Gilmore et al. 2012). We do the same here as a consistency check, but consider this not as robust as our previously described methods. When using all twins we obtain for the GCS-III an average metallicity of −0.13 ± 0.09 dex and temperature of 5702 ± 80 K, which confirms the previously found offsets in Section 3. Notice that two of our twins in Table 7 show very hot temperatures in C11. They have been marked (*) to have reddening that is not insignificant [$E(B-V) > 0.01$ mag]. The GCS assigns them to be 0.044 mag and 0.027 mag, respectively, despite the fact that they are only 50 pc away. Therefore it is possible that their reddening might have been overestimated for the C11 catalogue. A difference in reddening of $\Delta E(B-V) = 0.01$ corresponds to a change in temperature of $\Delta T_{eff} = 30$–50 K. If the stars are negligibly reddened, as their

Table 7. Our solar twins compared to the Sun. Note that the quoted solar $(b - y)$ is estimated indirectly from Sun-like stars by Holmberg et al. (2006). Stars marked with (*) may have poor temperatures, due to overestimated reddening corrections (see Section 4.4).

Name	$(b - y)$	M_V	[Fe/H] (GCS)	[Fe/H] (C11)	$T_{\rm eff}$(K) (GCS)	$T_{\rm eff}$(K) (C11)	Selection method
Sun (Holmberg)	0.403	4.83	0.00		5777		
Sun (this work)	0.409						
HD 76440*	0.419	4.82	−0.23	0.02	5623	5991	i, ii, n/i
HD 19641*	0.407	4.67	−0.19	0.00	5715	5928	i, n/i
HD 45184	0.394	4.67	−0.03	0.04	5821	5863	i, ii
HD 78660	0.409	4.75	−0.09	−0.03	5715	5788	i, n/i
HD 126525	0.426	4.94	−0.19	−0.10	5585	5666	i, n/i
HD 146233	0.404	4.79	−0.02	0.06	5768	5826	ii, n/i
HD 78538	0.407	4.95	−0.16	−0.09	5715	5781	ii
HD 183658	0.403	4.80	−0.01	0.06	5768	5826	ii
HD 197027	0.421	4.72	−0.24	−0.17	5610	5774	n/i
Average (all)	0.410	4.79	−0.13	−0.02	5702	5827	
Average (w/o dereddened stars)			−0.11	−0.03	5711	5789	

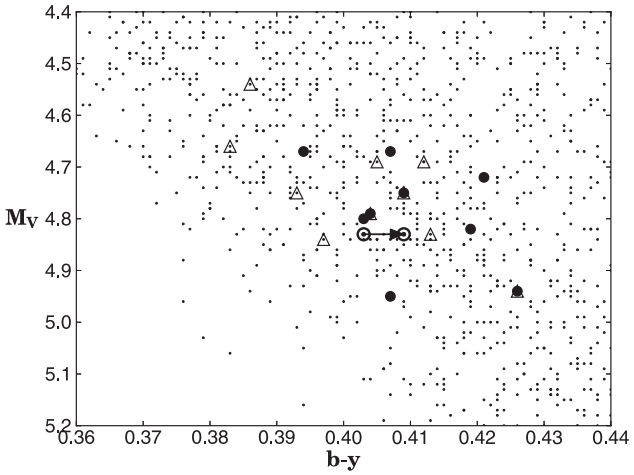

Figure 10. The colour–magnitude diagram for the GCS entries around the solar values (Nordström et al. 2004). The open triangles show the position of the solar twins we found in Paper I, and the filled circles are the twins from this study. The Sun is marked by the Sun symbol, using the colour values by Holmberg et al. (2006) for the left one, whereas the arrow is pointing to the position using our own determined value for $(b - y)$.

proximity would suggest, they are likely to be up to 200 K cooler than in C11. If we take out these two stars from the average, the new values are 5711 ± 86 K for the GCS and 5789 ± 63 K for C11, thus still favouring the latter calibration.

5 SUMMARY AND CONCLUSIONS

We have used several hundred weak neutral and ionized absorption lines for a range of atomic species to search for stars as similar to the Sun as possible ('solar twins') by comparing their spectra to a solar reflection spectrum of the asteroid Ceres.

In Paper I, we found offsets in the temperature and metallicity scales of the GCS, at least for solar-type stars, by using data from the FEROS instrument on the MPG/ESO 2.2-m telescope. Here we confirm the offsets, using more and considerably higher quality data, taken with the HARPS instrument on the 3.6-m ESO telescope. This makes us confident that these offsets are real, which are −55 ± 25 K in the temperature and −0.10 ± 0.03 dex in the metallicity scale for solar-type stars. These offsets are somewhat smaller, especially for temperature, than those in Paper I; but they agree within the errors. Note that one method we used in Paper I (the line depth ratio method) also indicated a smaller offset in temperature of about 50 K.

Note that all the errors quoted in the conclusions are averaged from the range of results among the different methods applied in this paper, which are discussed separately in the corresponding sections and are comparable to the internal errors of each method.

Our analysis favours the temperature and metallicity scale of C11 – explicitly tuned on solar twins – over the GCS-III values. We find small offsets of −13 ± 15 K in temperature and −0.02 ± 0.02 dex in metallicity around the solar values, which are within the error limits of our method.

In principle, the most fundamental test of the temperature scale is comparison with interferometry, but extant interferometric data do not yet allow for a strong conclusion about the GCS-III/C11 temperature calibration (Casagrande et al. 2014): the agreement of the two scales with interferometry is within 50 K or better, on the cool and hot side, respectively; the precise value of the offsets depending on the specific sample of interferometric stars considered for the comparison. Therefore, alternative tests of the temperature calibration remain useful. The one we presented in this paper and in Paper I has the advantage of relying on systematic trends established over a significant number of Sun-like stars.

From the HARPS data we also estimate the solar $(b - y)$ colour to be 0.409 ± 0.002, consistent with the $(b - y) = 0.403 \pm 0.013$ found by Holmberg et al. (2006), and close to what Meléndez et al. (2010) found: $(b - y) = 0.4105 \pm 0.0015$ and also close to what we found in Paper I: $(b - y) = 0.414 \pm 0.007$.

We also used this new set of data to further focus on finding solar twins. We found five new ones (HD 19641, HD 45184, HD 76440, HD 78538 and HD 183658), one that was only recently the focus of attention: HD 197027 (Freeman 2010) and confirmed all three twins in common with the sample of Paper I (HD 78660, HD 126525 and

HD 146233/18 Sco), guaranteeing consistency with our previous results.

As in Paper I, one of our best twins is HD 126525. This is a puzzle to us, as its temperature and metallicity values from the literature are very different from solar and our internal precision testing assigns to it values that are off by 100 K and 0.12 dex. We are currently analysing very high resolution and high S/N VLT/UVES spectra of this target to have a closer look at its elemental abundances to better settle the nature and parameters of this intriguing twin. It is also one of our targets which has a confirmed planetary companion (Mayor et al. 2011).

We demonstrate that the use of solar twins and solar analogues is an accurate and precise means of testing the stellar temperature and metallicity scales for Sun-like stars. Our methods in this paper and Paper I show a high degree of consistency and reliability, but have been applied so far only on the GCS catalogue. We plan to use these to test the calibrations of other scales for which temperature and metallicity estimates for solar analogues are available. It should be straight-forward to extend the applicability of our method beyond Sun-like stars, providing a way to probe any metallicity and temperature regime, by reference to a set of stars with accurate determinations of their fundamental parameters. In the past few years interferometric surveys have started to become that source of stars with parameters in the fundamental scale. Using these to anchor our methods to, we plan to probe other regions in the temperature–metallicity plane to provide a more global check of the calibration in spectro-photometric catalogues.

ACKNOWLEDGEMENTS

We are grateful to Johan Holmberg for originally suggesting to us the neutral/ionized method presented in this paper. We also thank our referee, Bengt Gustafsson, for constructive remarks. This study was financed by the Academy of Finland (grant nr. 130951 and 218317) and the StarryStory Fund. We thank Swinburne University, where part of this work was carried out.

REFERENCES

Allen C. W., 1976, Astrophysical Quantities, 3rd edn. Athlone, London
Bazot M. et al., 2011, A&A, 526, 4
Bazot M. et al., 2012, A&A, 544, A106
Bensby T., Feltzing S., Lundström I., 2003, A&A, 410, 527
Casagrande L., Ramírez I., Meléndez J., Bessell M., Asplund M., 2010, A&A, 512, A54
Casagrande L., Schönrich R., Asplund M., Cassisi S., Ramírez I., Meléndez J., Bensby T., Feltzing S., 2011, A&A, 530, A138 (C11)
Casagrande L. et al., 2014, MNRAS, preprint (arXiv:1401.3754)
Datson J., Flynn C., Portinari L., 2012, MNRAS, 426, 484 (Paper I)
Famaey B., Jorissen A., Luri X., Mayor M., Udry S., Dejonghe H., Turon C., 2005, A&A, 430, 165
Flynn C., Portinari L., 2006, MNRAS, 367, 449
Freeman K. C., 2010, Galaxies and their Masks. Springer Science+Business Media LLC, New York, p. 319
Gilmore G. et al., 2012, The Messenger, 147, 25
Holmberg J., Nordström B., Andersen J., 2007, A&A, 475, 519
Holmberg J., Nordström B., Andersen J., 2009, A&A, 501, 941
Kaempf T. A., de Boer K. S., Altmann M., 2005, A&A, 432, 879
Kaufer A., Stahl O., Tubbesing S., Norregaard P., Avila G., Francois P., Pasquini L., Pizzella A., 1999, The Messenger, 95, 8
Kiselman D., Pereira T. M. D., Gustafsson B., Asplund M., Meléndez J., Langhans K., 2011, A&A, 535, A14
Luck R. E., Heiter U., 2005, AJ, 129, 1063
Mayor M. et al., 2003, The Messenger, 114, 20
Mayor M. et al., 2011, A&A, preprint (arXiv:1109.2497)
Meléndez J., Ramírez I., 2007, ApJ, 669, L89
Meléndez J., Dodds-Eden K., Robles J., 2006, ApJ, 641, L133
Meléndez J., Asplund M., Gustafsson B., Yong D., 2009, ApJ, 704, L66
Meléndez J., Schuster W. J., Silva J. S., Ramírez I., Casagrande L., Coelho P., 2010, A&A, 522, A98
Meléndez J. et al., 2012, A&A, 543, A29
Monroe T. R. et al., 2013, ApJ, 774, L32
Munari U., ed., 2003, ASP Conf. Proc. Vol. 298, GAIA Spectroscopy: Science and Technology. Astron. Soc. Pac., San Francisco
Nordström B. et al., 2004, A&A, 418, 989
Palacios A., Gebran M., Josselin E., Martins F., Plez B., Belmas M., Sanguillon M., Lèbre A., 2010, A&A, 516, A13
Perryman M. A. C. et al., 1997, A&A, 323, L49
Skrutskie M. F., Skrutskie M. F., Capps R., 1995, BAAS, 27, 1392
Sozzetti A., 2004, MNRAS, 354, 1194
Takeda Y., Honda S., Kawanomoto S., Ando H., Sakurai T., 2010, A&A, 515, A93
Torres C. A. O., Quast G. R., da Silva L., de La Reza R., Melo C. H. F., Sterzik M., 2006, A&A, 460, 695
van Leeuwen F., 2007, A&A, 474, 653
York D. G. et al., 2000, AJ, 120, 1579

This paper has been typeset from a TEX/LATEX file prepared by the author.